CHAPTER 1

INTRODUCTION

1.1 Vertical seismic profiling (VSP)

The geometry of the VSP survey separates the method from other types of borehole and surface related surveys. The surface seismic survey is conducted with the geophones (or hydrophones in the case of marine seismics) and the sources being on or near the surface. In crosswell seismology or CWS (Hardage, 1992), both the sources and receivers are in boreholes. For the reverse VSP (RVSP; Hardage, 1992), the source is in the borehole and the receivers are on the surface. The VSP technology, data and interpretation presented in this thesis relate to a survey with sources on the surface and receivers in the borehole.

How has the VSP survey been doing in comparison to the other seismic surveys? Recently, Zimmerman and Chen (1993) ranked the VSP to yield superior interpretable data from deeper depths in comparison to the RVSP results. The viability of RVSP and CWS data will closely follow the development of the downhole seismic sources (Hardage, 1992). The downhole geophone tool (sonde) used in the VSP survey is operated in a seismic environment which involves less background noise in comparison to the surface geophone (RVSP and surface seismics). The locking arm on the sonde has changed from spring loaded (a derivative of the caliper tool) to being hydraulically operated (enough force to almost bend steel borehole casing). The increased level of geophone coupling to the formations surrounding the borehole increases the seismic signal reception (Hardage, 1985). Multi-level geophone sondes with independent locking arm units have resulted in a reduction of VSP survey cost and less coupling resonances.

What has happened in the past with respect to interpretation? In theory, as explorationists, we would like to integrate the interpretation of the VSP data with the processing of the same data. In this way, both activities would complement and guide each other. In practice, however, they seem to be done separately. This may be due to time constraints placed on the seismic interpreter as a result of heavy work load or to the specialization of the interpreter and the processor to one or the other task. First, the VSP data are usually processed using whatever methods are available to the processor. The processing typically proceeds to output a product which is the separated upgoing wavefield events in pseudo-two-way traveltime. Thereafter, the interpreter takes the final result data panel and, in conjunction with available geological data, interprets the different VSP events. Unfortunately, the interpretation is usually done in the absence of input from the processor. The insight of at least the first pass of the processing has been lost to the interpreter.

1.2 Aims and objectives of this study

The aim of this thesis will be to:

(1) develop the methodology of Interpretive Processing (Hinds et al., 1989a) for VSP data using the interpretive processing panels (IPP), interactive data processing, integrated log display (ILD), integrated seismic display (ISD) and the integrated interpretation display (IID);

(2) review the usage of the processing steps in the individual IPP to illustrate the incorporation of VSP interpretation to minimize processing artifacts (Hinds et al., 1994c);

(3) present the usage of VSP interpretive processing in four case studies (Hinds et al., 1989a; Hinds et al., 1993b, 1994a and 1994c; Hinds at al., 1993a and 1994b; Hinds et al, 1993c); and

(4) further the method of integrated geophysical/geological interpretation (Anderson, 1986) using the case studies (Hinds et al., 1989a; Hinds et al., 1991a, 1991b and 1993c; Hinds et al., 1993a and 1994b; Hinds et al., 1993b, 1994a and 1994c).

The integrated processing and interpretation of VSP data will be developed to work together in order to enhance the final VSP interpretation. Furthermore, the interpretive processing of the VSP data within the case histories will be reviewed along with the usage of the final

VSP results (both near and far offset data) into the integrated geological/geophysical interpretations presented in the case studies. This thesis will attempt to personify the term "interpreter/processor" as first highlighted in Hardage (1985).

The case histories pertain to oil and gas exploration in carbonate reef and sandstones in the Western Canadian Sedimentary Basin (WCSB). The Lanaway case history (Hinds et al., 1994a) described in chapter 3 pertains to the exploration of the Lanaway/Garrington oil field located in central Alberta, Canada. The surface seismic interpretation over the reef crest differed dramatically from the isopach of the reef-encasing shales derived from the geological logs of a borehole drilled into the reef crest. To understand the discrepancy, a VSP survey was performed and the data were interpretatively processed. The results were integrated with the known geology of the field area to uncover possible reasons for the surface seismic anomaly.

The Ricinus case history (Hinds et al., 1993c) described in chapter 4 is a study in reef hunting within the Ricinus field in central Alberta, Canada, using the far offset VSP survey. Existing surface seismic was used to infer that a well drilled into the interpreted North-east corner of the Ricinus reef would be successful in penetrating oil bearing carbonate reef. The well was drilled; however, the well missed the reef and a near and far offset VSP survey was used to seismically image possible reef buildups in an area around the well.

The Fort St. John Graben case history (Hinds et al., 1991a; Hinds et al., 1993a) described in chapter 5 highlights exploration of a gas-filled channel sandstone using near and far offset (lateral) VSP surveys. An exploration well was drilled within the study area which intersected the target zone sandstone (the basal Kiskatinaw of the Upper Carboniferous). The target sandstone had a high shale content and was not reservoir quality. A near offset and two far offset VSP surveys were run in the exploration well to image out to a distance of 350 m to the North-west and to the East of the well. The VSP, surface seismic and geology results (from the geological logs of the exploration and surrounding wells) are integrated to infer a clearer picture of the sand/shale relationships of the basal Kiskatinaw and detailed faulting of the Carboniferous strata around the well and within the surface seismic line area.

The Simonette field case history (Hinds et al., 1991b; Hinds et al., 1993b) described in chapter 6 involves using VSP results to image the slope of a low-relief carbonate reef. The low-relief reef examined using the VSP data is located at the extreme end of a North-east reef spur of the Simonette Reef located in North-west Alberta, Canada. An exploration well drilled in the low-relief reef penetrated the edge of the reef. The VSP surveys were run in order to infer details of the reef slope. The interpretation of the VSP data was integrated with all other exploration data to infer the location of the crest of the low-relief reef and to assist in determining whether to whipstock the exploration well or not.

1.3 Acknowledgements

The thesis contains a variety of datasets and the processing has been performed at a number of facilities using different processing software. The surface seismic and VSP data examined in chapters 3 and 4 were donated by Gulf Canada Ltd. (Hinds et al., 1989a). The surface seismic and VSP data for chapters 5 and 6 were donated by Talisman Resources Inc.

The surface seismic data used in the thesis case histories consisted of post-stack seismic time sections. The VSP data were the raw data; re-processing was then performed on the data. The subsequent processing for the VSP data shown in this thesis was different to that of the industry standard processing at the time of data acquisition.

The VSP processing was performed on the computers of Computalog Ltd. (Calgary) using Halliburton Geophysical Inc. software, on the VAX systems at the University of Pretoria, Talisman Resources Inc. (Calgary) and Anglo-American Prospecting Services (Klerksdorp), using IT&A Insight/1 software and on the Schlumberger computers using Schlumberger propriety software in Paris, France. Rick Kuzmiski taught me the Halliburton software in Calgary and Didier Belaud performed the Kirchhoff migrations shown in the thesis during my research stay in Paris as I was not allowed physical access to the Schlumberger machines. Much of the VSP processing for the work described in chapters 2 and 4 were done using Photon Systems Ltd (Calgary) Quickpro software resident on my 486 DX/2 PC in Pretoria.

The well logs used during the construction of the isopach map and geologic cross-section shown in Figures 6.1 and 6.2 were supplied by Karen Chang of Calgary. The initial interpretations of the surface seismic sections were supplied by the data owners; however, all subsequent interpretations were done during this research. The design of the VSP surveys and supervision of the execution of the field surveys were done by myself as an employee of Gulf Canada Ltd. and as a consultant for Hinds Geophysical Inc. (Calgary).

I would like to acknowledge and thank my supervisors, Prof. C.P Snyman, Dr. N.L. Anderson and Dr. R. Kleywegt for their help and interest in this thesis work.

1.4 VSP fundamentals

1.4.1 Near and far offset (lateral) VSP surveys

The components of the interpretive processing panels are different for the near and the far offset VSP surveys. The near offset VSP survey usually involves the processing the vertical (Z) axis geophone data; whereas the two horizontal (X and Y) and vertical (Z) geophone data are processed for the far offset VSP survey.

A review of the geometries involved in the VSP survey which necessitate the different panel components will be discussed below. A few of the numerous configurations of the VSP survey are shown in Figure 1.1 (Hinds et al., 1989a). A near offset VSP geometry can be described as the source being vertically or near-vertically above the sonde. The near offset VSP has also been termed a "zero offset" VSP survey (Cassell, 1984). In Figure 1.1, the configurations in part (A) using the source S_1 and in (B) using the source S_4 and sonde at location C plus the source S_3 and receiver at location A would be termed near offset VSP source-receiver geometries. The configurations in (A) using the source S_2 and in (B) using the source S_3 and receiver at B or C would be termed far offset VSP (or simply "offset" VSP; Cassell, 1984) geometries.

The far offset VSP geometry for a deviated hole could arise in an offshore well where the airgun is placed near to the drilling platform but the wellbore is deviated to intersect reservoirs quite a distance away from the subsurface location directly below the well.

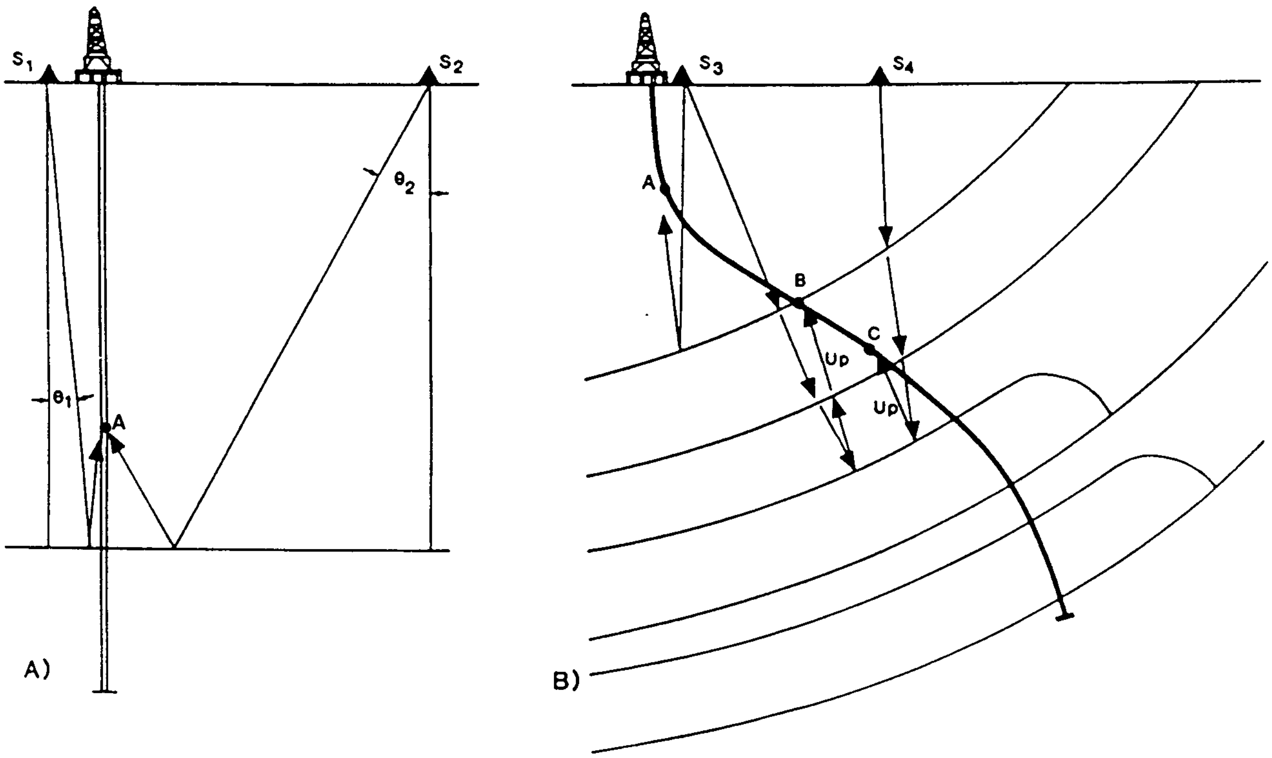

Figure 1.1 The field layout of the (zero) near and far offset VSP surveys. In part (A), the surface source at S_1 is at a zero-incidence location with respect to the geophone borehole sonde in the vertical non-deviated borehole. The up- and downgoing waves travel vertically down to the reflector and back to the receiver geophone sonde in the borehole. The source at S_2 is a non-zero offset location as the source does not lie directly over the borehole geophone. In part (B) for the deviated borehole, source S_3 is in a zero-offset configuration for the upper vertical (shallow depths) part of the borehole and (non-zero) far offset for the deviated remainder of the borehole. Part (B) is usually represented in the literature as a deviated borehole intersecting horizontal layers which would result in incorrect reflection angles for the migration algorithms (from Hinds et al., 1989a).

In the case where the borehole is deviated but a near offset geometry is desired, the source is moved along the surface and is directly overhead of the sonde within the borehole. This is obviously an expensive procedure as the three-dimensional picture of the location of the sonde must be monitored. The source would move once the "verticality" of the source-receiver geometry needed to be corrected (remember that the Fresnel zone concept relates both to the receiver and source; Hardage, 1985). In land-based VSP surveys, retaining the zero offset geometry can be difficult because bush corridors must be cut and large Vibroseis vehicles may need to be "sledded" over to source locations.

The interpretational definition that I like to use is that a far offset geometry exists whenever partitioning a wavefield (downgoing or upgoing P- or SV-waves) necessitates the polarization of the VSP data in order to isolate that wavefield component onto a single data channel (following an angle-based rotation). In a far offset VSP, reflected and transmitted P, SH, and SV-waves (Fig. 1.2) will be recorded by the sonde with the amplitudes of the various waves being related to the incidence angle onto the geophones.

1.4.2 Primary and multiple up- and downgoing waves

The VSP data contains upgoing and downgoing waves (Fig. 1.3) which can have a variety of origins. Figure 1.3A shows example raypaths of the primary and multiple up- and downgoing waves. Using two interfaces (A and B), Figure 1.3B depicts the location of the VSP events on a depth versus traveltime diagram.

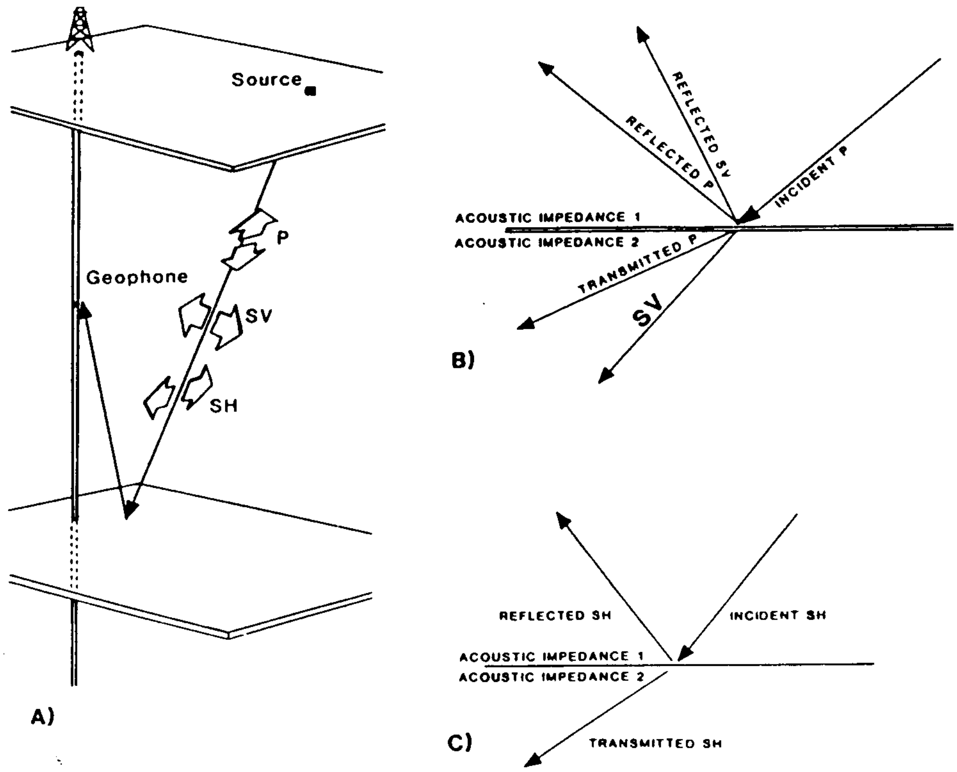

Figure 1.2 The up- and downgoing waves propagating to the wellbore geophone sonde can be compressional P-waves that vibrate in the direction of travel or Shear SV- or SH-waves that vibrate normal to the direction of travel, either in the plane of the source and receiver or out of the plane. Reflections from dipping and contorted geological strata can enable all three of these type wavefields to be recorded on the X, Y, and Z geophones. As shown in part (B), the P- and SV-waves can reflect and transmit as P- or SV-waves at impedance interfaces. The SH incident wave reflects and transmits as an SH wave (C). (from Hinds et al., 1989a).

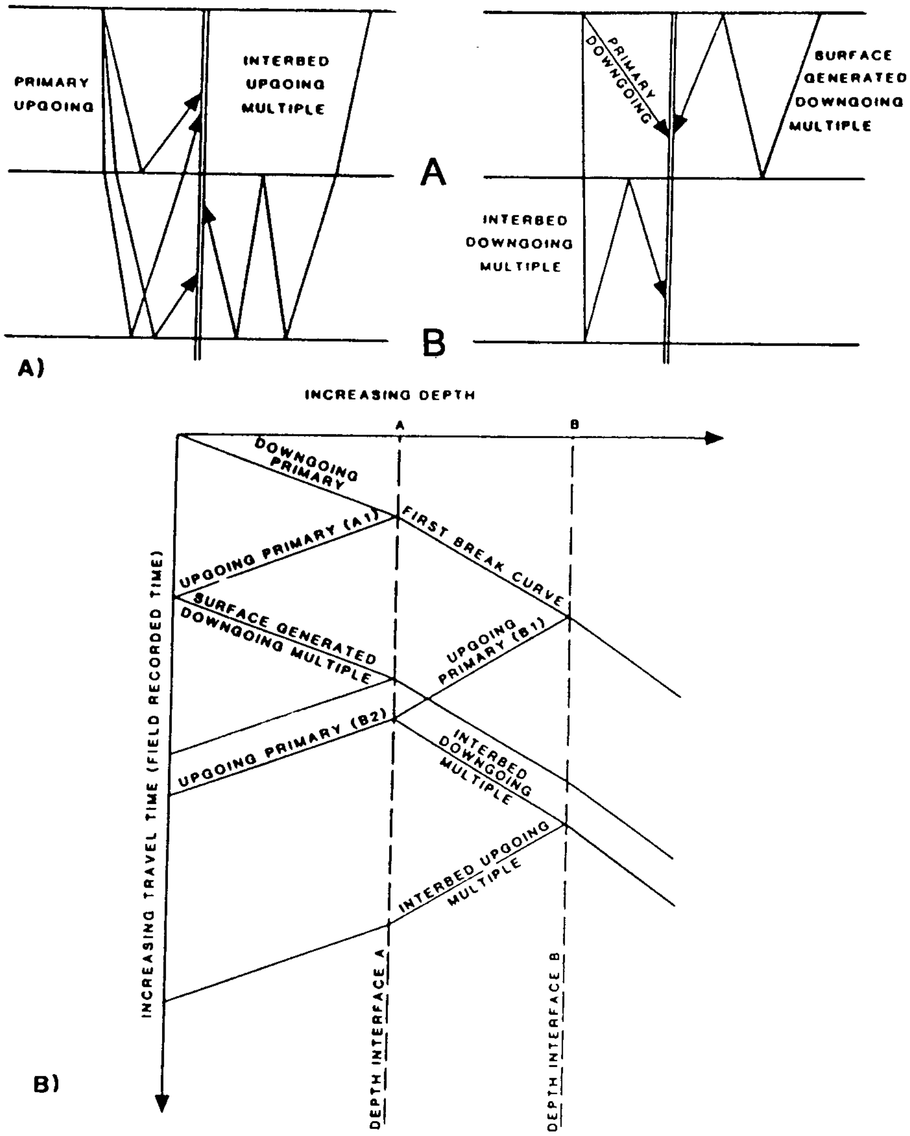

Figure 1.3 Examples of the up- and downgoing raypaths (A) and depth-traveltime diagrams (B) for both primary and multiple reflections. The upgoing rays are illustrated on the left side of (A) whereas the downgoing rays are illustrated on the right side. The geometry for the near offset sources are displayed with exaggerated source offset for clarity. The surface-generated downgoing multiples will be recorded at all subsurface geophone locations whereas the interbed downgoing multiple generated between layers A and B will only be recorded when the geophone is below layer A. Upgoing reflections from layer A will be recorded only at geophone locations above layer A. The up- and downgoing primaries will merge when the geophones are located at the generating interface. A traveltime curve plot for the up- and downgoing rays is shown in part B. The downgoing primary is the first break curve increasing in traveltime from left to right in the diagram and with the exception of head waves is the first recorded signal on each VSP trace. The downgoing wave multiple for the near-offset case parallel the downgoing primary. An upgoing primary (B1) generates a reflected downgoing multiple at interface A, which in turn can generate an interbed upgoing multiple at reflector B (from Hinds et al., 1989a).

Throughout the thesis, the abbreviations FRT, -TT, and +TT (Hinds et al., 1989a) are used repeatedly. FRT is the abbreviation for field recorded time, the term used to describe the time-depth display of the raw field records. FRT include time recording shifts input by airgun delays or Vibroseis recordings. The terms -TT and +TT refer to specific data configurations following trace time shifts. -TT is used in reference to the display on which the first breaks and downgoing P-waves are horizontally aligned and bulk shifted. On these displays, the first break times have been subtracted from each trace, and the modified traces have been bulk-shifted to an arbitrary time-datum (usually to 100 to 200 ms) so that the onset of the first break wavelet is retained. +TT is used in reference to the display on which the first break time of each trace has been added to that trace (plus possible normal moveout or "NMO" corrections), as depicted in Figure 1.4. On the +TT displays, the upgoing events on near offset VSP data are horizontally aligned and should be in pseudo-two-way traveltime.

For the near offset VSP data, one of the important types of events to interpret are the surface-generated and interbed multiples. The ease with which primaries and multiples can be identified was reviewed in early papers by Wuenschel (1976) and Kennett et al. (1980). Some fundamental guidelines for VSP interpretation were set down in the literature in Hardage (1985). The significance of multiples for Western Canadian Sedimentary Basin (WCSB) VSP data was shown in Hampson and Mewhort (1983) and Hinds et al. (1989a).

For the surface-generated multiple, the downgoing wave reflects at an interface and then reflects from the surface back down towards the borehole geophone. The key to the interpretation of the surface-generated multiple is that it must reside on all the VSP traces. Later, in Chapter 2, when the VSP data are placed in the -TT configuration the surface-

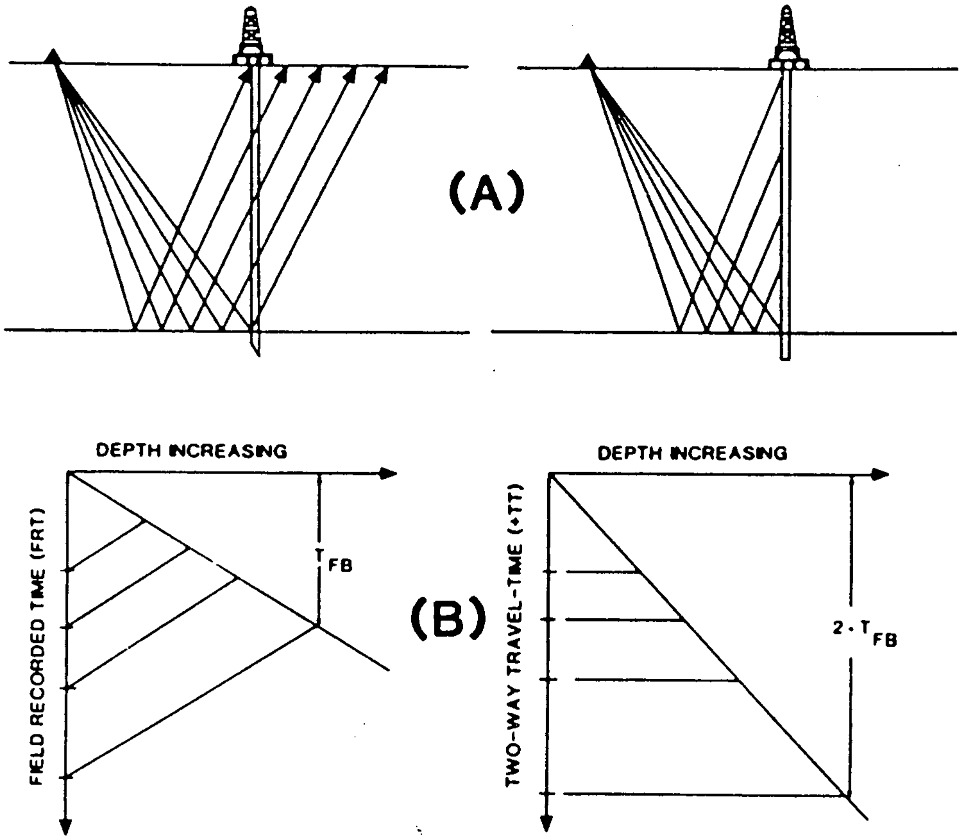

Figure 1.4 The near offset data correction used to place the data into pseudo-two-way traveltime (+TT). Part (A) shows the geometry of the surface seismic with the well superimposed on the raypaths. To the right, the rays that are terminated at the well are different from the surface seismic rays by a traveltime equivalent to the zero-offset first break times of the downgoing rays. In part (B), when the first break traveltimes are added back onto the traces, the time axis changes from field recorded time (FRT) to pseudo-two-way traveltime (+TT) that should be equivalent to the surface seismic two-way traveltime (from Hinds et al., 1989a).

generated multiple will become easily interpretable. The simple corollary to this is that the first break curve shown in Figure 1.3 is the only primary downgoing P-wave on the VSP. It should be noted that if the mode converted P-SV downgoing wave is created at interface A in Figure 1.3, then that mode-converted downgoing wave will also be a primary downgoing wave. Since the only primary downgoing P event is the P-wave event associated with the first break, then later arriving downgoing P events recorded at the sonde are multiples.

Why is this simple information not seen on surface seismics? The answer is that no downgoing waves are recorded by the surface seismic geophones. By placing the VSP data into the +TT data configuration, however, the interpretation of multiples on surface seismics can be facilitated. Figure 1.5 depicts the VSP interbed multiple. As seen in Figure 1.3, the interbed multiple exists as a downgoing wave only below the top generating interface that is responsible for the multiple's existence. The upgoing interbed multiple exists only on the shallowest VSP trace down to the trace recorded at the bottom generating interface. Can these two observations be combined to find a simple way to interpret the interbed multiple? In Figure 1.5, the upgoing wave (+TT) VSP data show that the upgoing interbed multiple mimics the upgoing primary (U-P) from the interface from Z_2 but is delayed by the two-way traveltime between the interface at Z_1 and Z_2. The other observation which is also used in designing corridor stacks in chapter 2 is that the interbed (or any other) multiple does not intersect the first break curve. Figure 1.3 shows that the upgoing interbed multiple can be mistaken as a surface-generated multiple if a downgoing surface-generated multiple was created with the same time delay as the time difference between the upgoing primary associated with Z_2 and the multiple seen below the Z_2 primary (U-M in Fig. 1.5A). The

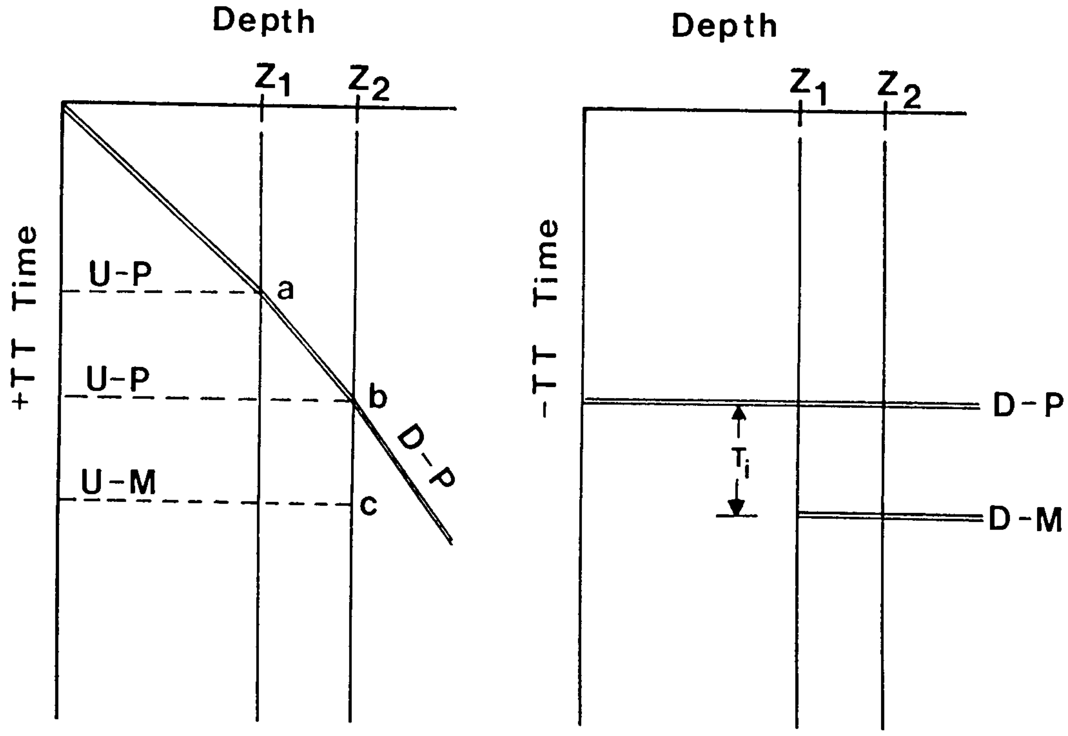

Figure 1.5 Upgoing wave events in (+TT) time (left) and downgoing waves in (-TT) time (right) are displaced to align the upgoing primary event generated at the depth Z_2 (labelled U-P on the left) with the horizontally aligned event first break curve (labelled D-P on the right). This illustrates the equal time separation (T_i) between the U-P and U-M events from interface Z_2 and the D-P and D-M downgoing events.

interpretation is clarified by viewing the (-TT) downgoing events as shown in Figure 1.5B. A downgoing multiple (D-M) is recorded after the primary downgoing wave (D-P) and exists only below the Z_1 interface.

Can the downgoing waves be used to attenuate the upgoing wave multiples? Hubbard (1979) and Gaiser et al. (1984) showed that a deconvolution operator which could collapse the downgoing event wavetrain into a single pulse could be used to attenuate the upgoing multiples. In Figure 1.6 (Hardage, 1985), there is a constant time shift, T_m, between the upgoing primary and multiple and downgoing primary and multiple. The up- and downgoing multiples are linked to their respective primary events by this constant time shift. Since the upgoing wave is the same as the downgoing wave at an interface, an operator designed from the downgoing waves will be able to attenuate the corresponding upgoing wave multiples. In practice, this procedure of using a single deconvolution operator works well with surface-generated multiples.

In Figure 1.5, it can be seen the interbed multiples do not appear on all VSP traces. This implies that independent deconvolution operators would have to be calculated for each VSP trace in order to attempt to combat the interbed upgoing multiple. The multiples that occur after the first break time of the deepest geophone are also difficult to attenuate (one reason being that these events cannot even be confirmed to be multiple or primary events).

For the interpretive processing of near offset VSP data, such an importance is placed on identifying multiples that 75% of the interpretive processing panels have been designed to evaluate the performance of the "up over down" VSP deconvolution procedure. As will be

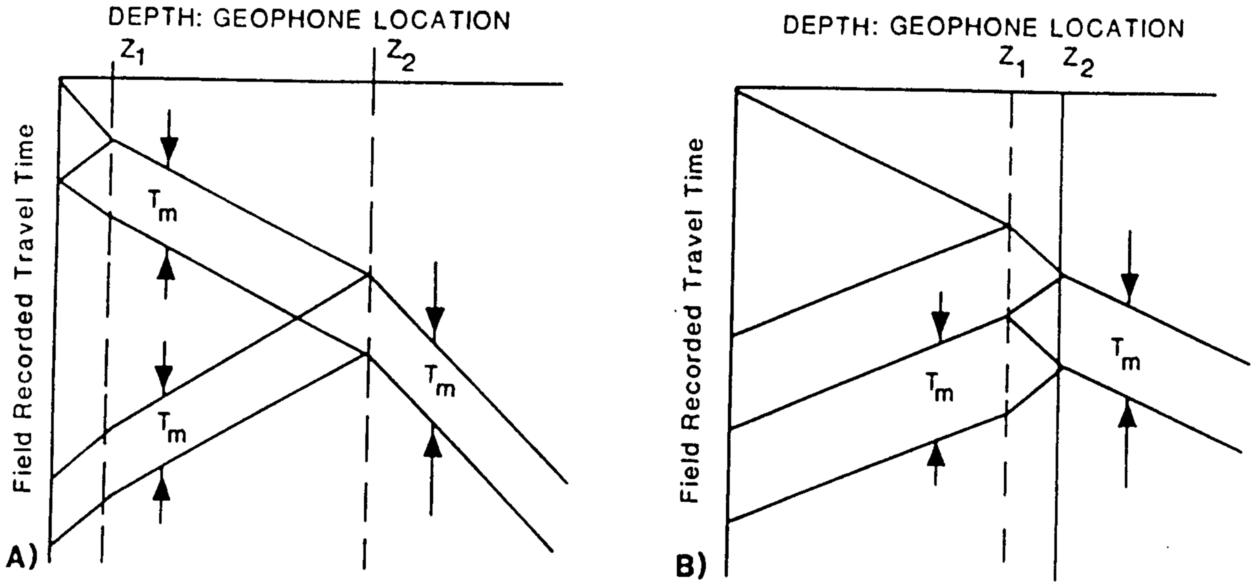

Figure 1.6 The constant time shift between the up- and downgoing primaries and multiples for the surface-generated (A) and interbed multiples (Hardage, 1985). Part (A) is the depth versus FRT configuration for the surface generated multiple. The numerical operator (inverse filter) that attenuates the downgoing multiple (the downgoing event that is time shifted from the primary downgoing event by time Tm) will attenuate the upgoing surface generated multiple. In part (B), the operator that will attenuate the upgoing interbed multiple can be designed from any trace beneath depth location Z_1 (from Hinds et al., 1989a).

seen on the modelled VSP data later in this chapter, the crucial key to multiple attenuation is that the constant time delay between the up- and downgoing multiple events and their associated primary events is preserved on the entire VSP dataset. When the offset of the source begins to approach far offset, the key time lag assumption becomes violated and deconvolution of far offset VSP data may not always work.

Figure 1.7 depicts near offset VSP results of a four layer model illustrating surface-generated multiple contaminated data (panel 1) and interbed multiple contaminated data (panel 2). Compare the modelled results to the schematic VSP events shown in Figure 1.3B. Here a short review is included to show how an interpreter/processor pulls apart the different events that one would see on the modelled (simulating a real) VSP data.

Consider panel 1 of Figure 1.7. The horizontal axis reflects the depth of the recording sonde (in m) and the vertical axis is in the **FRT** time configuration (in s). The first downgoing wave is recognized as the first break on every trace and as the depth increases, the traveltime of the downgoing event also increases (the basic rule for a downgoing VSP event). The downgoing primary wave encounters an acoustic impedance interface at 120 m depth and an upgoing primary event is generated due to the reflection. The upgoing primary intersects the primary downgoing event on the 120 m trace at approximately 0.5 s. The upgoing wave traveltime increases with decreasing depth. This shows the familiar relationship that for the near offset VSP the up- and downgoing events have equal but opposite apparent velocities (Hardage, 1985). At 0.9 s on the surface trace, the upgoing event is turned into a downgoing surface-generated multiple due to the reflection of the upgoing wave at the

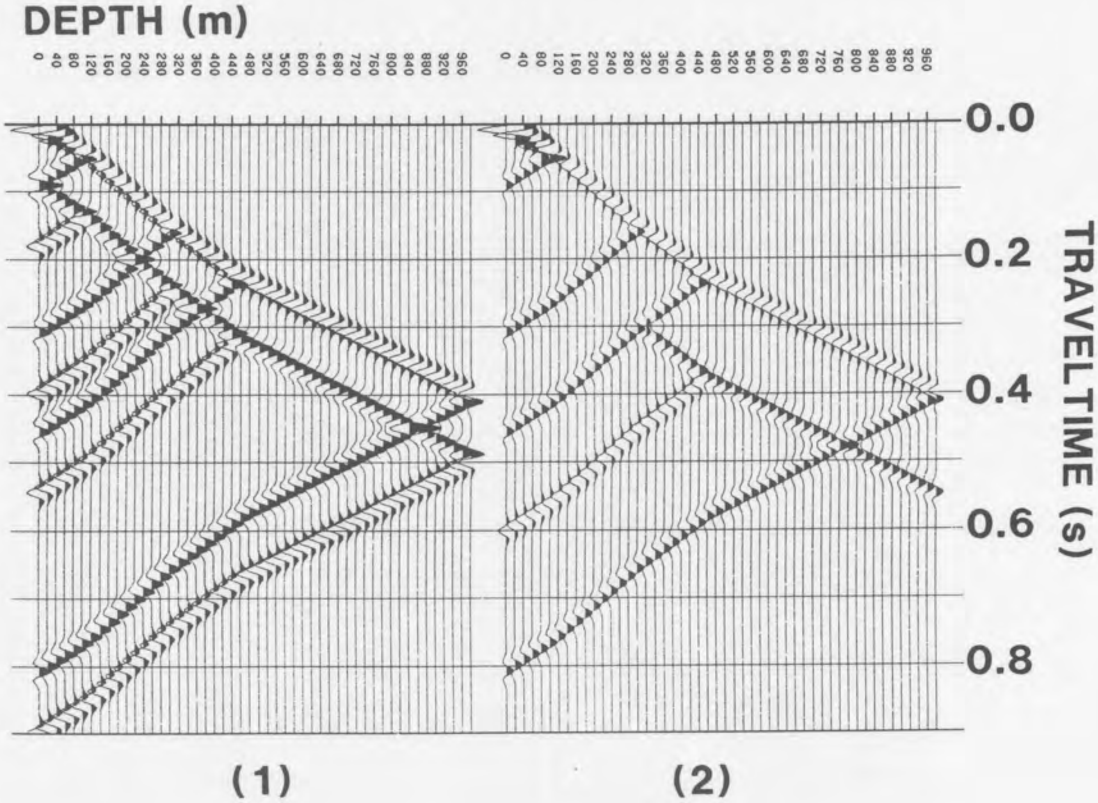

Figure 1.7 Synthetic VSP seismograms illustrating surface generated (panel 1) and interbed (panel 2) up- and downgoing multiple events. The model used in the ray tracing consisted of four layers with the half space being at the bottom of the borehole. The trace spacing is 20 m. The geometry consists of a near-offset source and a vertical non-deviated borehole. The amplitudes have been equalized and the first arrival on the 0 m trace has been muted for clarity. Note the differences in the location of the up- and downgoing multiple events and the polarity reversals between the various up- and downgoing wave events (from Hinds et al., 1994c).

surface. The downgoing multiple travels back down to the interface at 120 m, transmits downwards as a downgoing multiple and reflects back up to the surface as the first upgoing surface-generated multiple. The other upgoing multiples can thereafter be similarly traced.

The interpreter/processor must get a good understanding of the events on the raw VSP (possibly by gaining the VSP or by separating the up- and downgoing events, amplitude gaining the events independently, and thereafter recombining the two datasets for interpretational reference - REMIX display; Hinds et al., 1989a) as this will lead his interpretive processing right through to the final displays.

The surface-generated downgoing multiple in Figure 1.7 (panel 1) is time delayed from the primary (first break) downgoing event by the time that the downgoing wave took to reach the first interface at 120 m depth and travel back (as an upgoing wave) to the surface. As noted above, the multiple exists on all of the VSP traces. It is clear, visually, that the constant time shift between the downgoing primary and multiple corresponds to the same time delay between all of the upgoing multiples and their respective upgoing primaries.

In panel 2, the interbed up- and downgoing multiples are generated at interfaces 2 and 3 (320 and 480 m depth, respectively). As noted above, the downgoing interbed multiple exists on traces recorded deeper than the top generating interface (at 320 m depth) and the upgoing interbed multiple exists on traces above the 480 m interface (the bottom generating interface). This key to interpretation may be difficult to recognize when using downgoing wavefield separation techniques that smear the downgoing multiple events across adjacent traces.

For interpretative processing, the objective is to first identify the multiples and then to attenuate them the best possible. If attenuation is not completely possible then the knowledge of the multiple contamination must be included in the evaluation of the data.

1.4.3 Far offset geometries

The triaxial geophone sonde is usually employed in a far offset survey; however, there are cases where the near offset VSP survey requires the recording of the **X**, **Y** and **Z** channel data. Shear waves can be generated using shear wave Vibroseis units or through mode conversion at near surface interfaces. When the shear wave passes through vertical fractures (Fig. 1.8; Ahmed, 1989 and 1990), the shear wave can be polarized and split into two resultant shear waves; one which is oriented normal to the fractures and the other parallel. These fast and slow shear waves that exist below the fracture zone would be recorded using a triaxial geophone sonde even though the source could have been located at the well (a near offset source). Another example of a case where a triaxial sonde is required is within the near offset VSP geometry shown in Figure 1.9. The object in this survey is to image the steeply dipping target horizon and to locate the fault. The reflected waves from the target horizon would require a triaxial recording to properly image the horizon. In these cases, the geometry of the target or rock properties themselves are causing orientation changes within the transmitted or reflected wavefields. At any given sonde location, three channels of data are recorded; namely the **Z**, **X**, and **Y** axis data. The **X** and **Y** channels are from the two

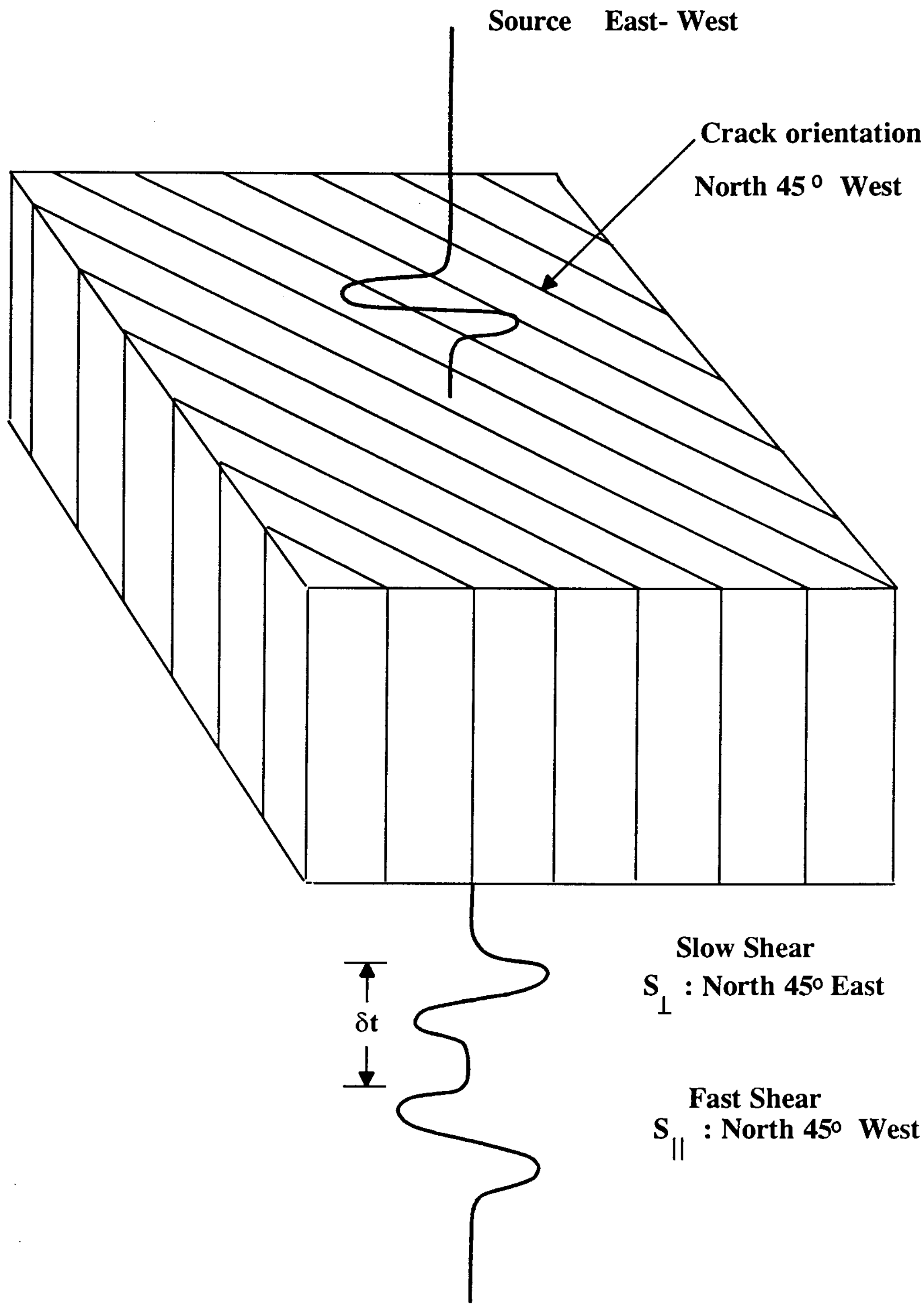

Figure 1.8 Schematic diagram of shear wave splitting caused by the propagation of a SV wave through fractured rock. This type of wave propagation would complicate the waveforms recorded at the triaxial geophone sonde (from Ahmed, 1990).

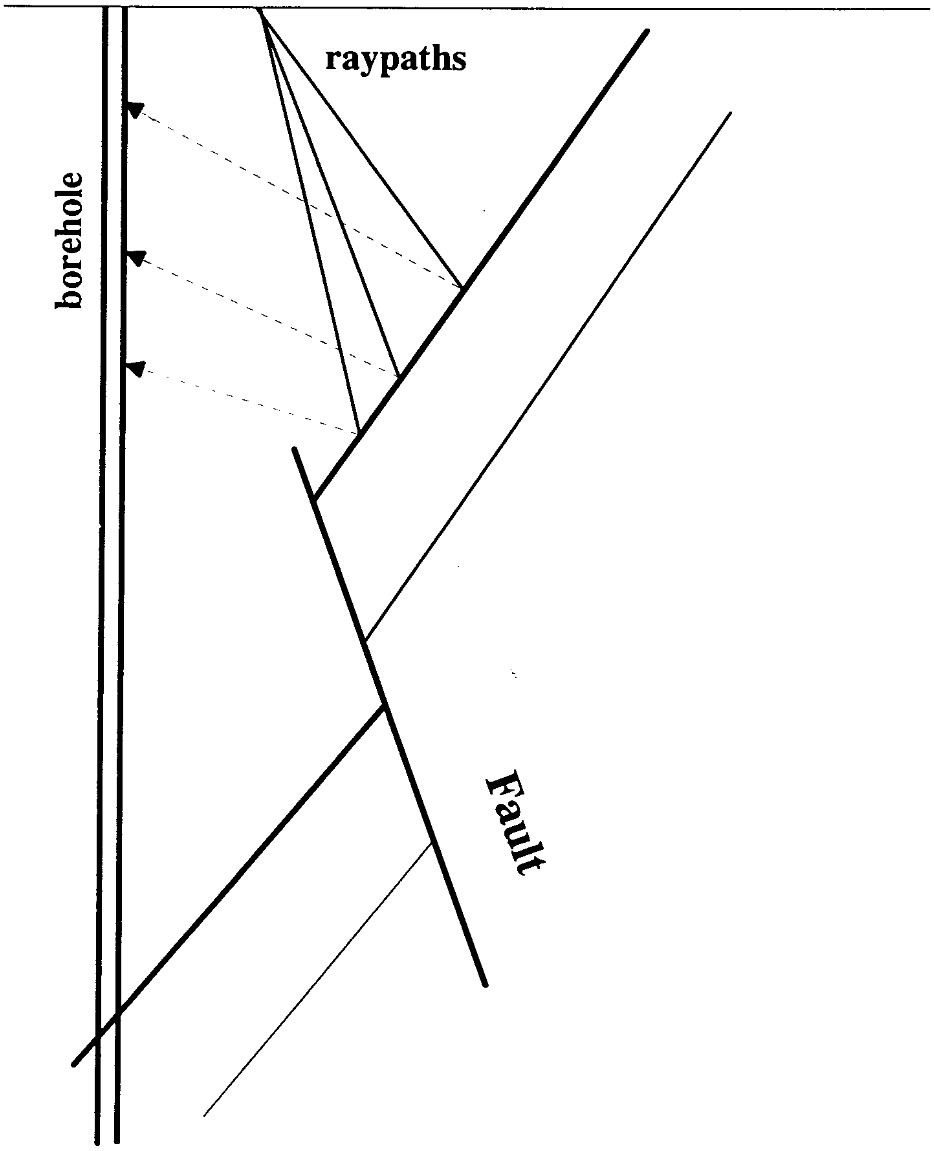

Figure 1.9 From a near offset source, reflected rays propagate to the borehole along complicated paths due to the steeply dipping geology. This would result in the triaxial data requiring special polarization analysis in order to interpret the VSP reflections.

orthogonal horizontal geophones.

As the sonde is raised up the borehole, the horizontal geophones rotate in the borehole. The vertically and horizontally polarized shear wavefields, SV and SH (Bullen and Bolt, 1985), and the compressional P-wavefield energy are contained in varying amounts on the **X** and **Y** data channels.

The first objective when processing triaxial data is to isolate the downgoing P-wave events from the **X** and **Y** channels onto a single data panel. The procedure to do this involves data polarizations which are explained below.

For the far offset VSP surveys, the hodogram analysis (Hardage, 1985; DiSiena et al., 1984) performed on the first break wavelets of the two horizontal datasets (from the same sonde location) can be used to polarize the **X** and **Y** data onto two principal axes normal, **HMIN**, and tangential, **HMAX**, to the plane defined by the source and the well (Fig. 1.10). The resultant **HMIN** and **HMAX** data should contain polarized SH and combined P and SV energy, respectively. The assumption for SH- and SV-wavefield separation is that the two waves are propagated along a similar raypath to the downgoing P-wave (Hardage, 1985).

The hodogram method polarizes the horizontal axis data using the downgoing P-wave energy in the first break wavelet. A time window around the first break is chosen and the data from the two horizontal channels are plotted on an orthogonal axis. For any given time sample in the window, the corresponding **X** and **Y** values are plotted on the graph called a hodogram (Hardage, 1985; Fig. 12.24 of Hinds et al., 1989a). The hodogram usually resembles an

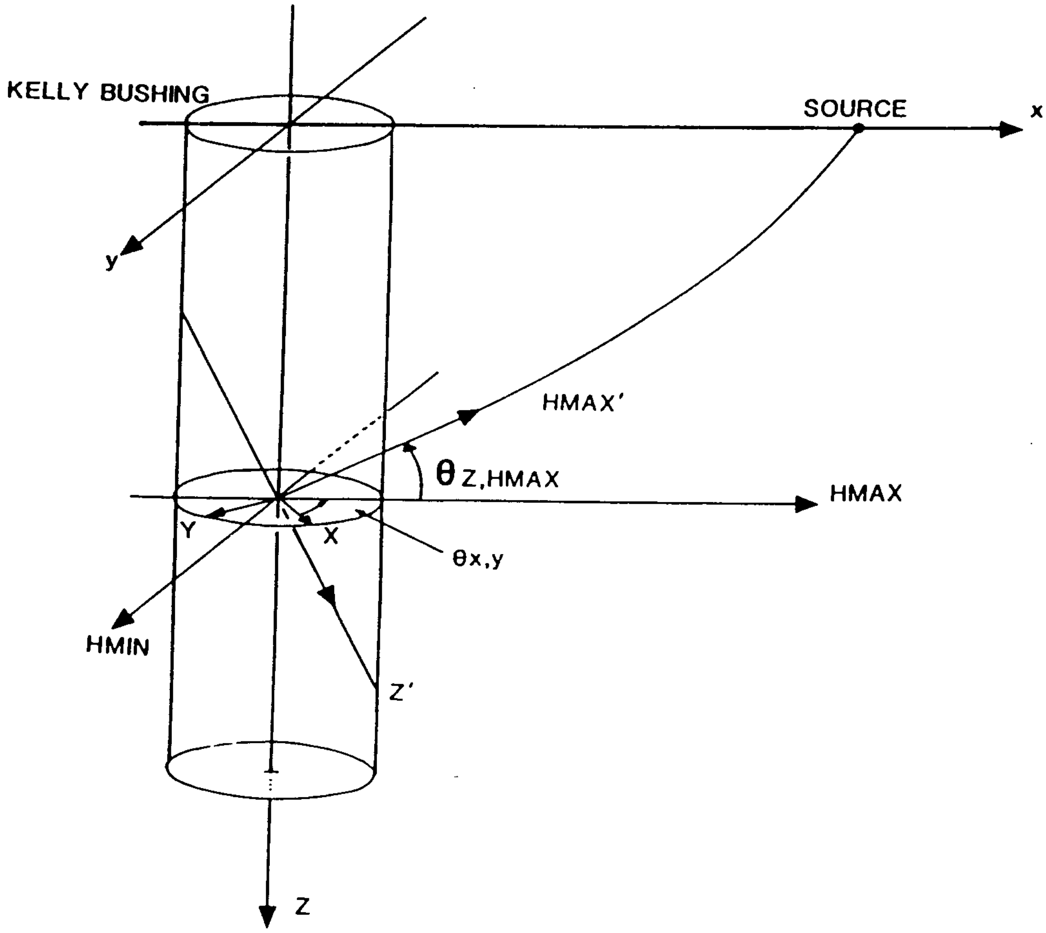

Figure 1.10 The orthogonal coordinate system of the local **X**, **Y**, and **Z** geophones along with the coordinate axis (**HMIN**, **HMAX**, **Z'** and **HMAX'**) that will be used as the principal axis in the hodogram (non-time variant) analysis (from Hinds et al., 1989a)

ellipse pointing in the direction of the azimuth of the incoming downgoing wave. The angle found in the hodogram analysis is used in a non-time variant rotation matrix equation where the input traces plus the rotation matrix are used to calculate the **HMIN** and **HMAX** traces (see Appendix). The output data will be the **HMAX** panel which contains SV and P-wave energy. For normal purposes, the **HMIN** data are discarded.

The **HMAX** and **Z** data are assumed to be orientated in the plane defined by the well and the source. The second objective is to use hodogram based polarization on the **Z** and the **HMAX** data. The **Z** and **HMAX** data are processed to output the **Z'** and **HMAX'** data using the rotation angle found during a hodogram analysis of the input data. The **HMAX'** data are assumed to predominately contain downgoing P-wave events and upgoing SV-wave events. In chapter 2, the inputs and outputs of the various polarizations are shown and an IPP is developed to ensure data processing quality for the procedures.

Does the geometry play a role in the polarizations? In Figure 1.11, the sonde axes in a deviated borehole and three different source locations are shown. The amount of partitioning onto the various axes can vary significantly depending on the source-receiver geometry within the deviated borehole. The objective with the two rotations, however, is achieved using normal hodogram analysis. The **HMAX'** data panel contains predominately downgoing P and upgoing SV-wave energy and the **Z'** axis data contains downgoing SV and upgoing P energy (Fig. 1.12).

If the up- and downgoing wave particle motion were exactly orthogonal then no further event partitioning processing is necessary. The **Z'** axis data panel would be interpreted following

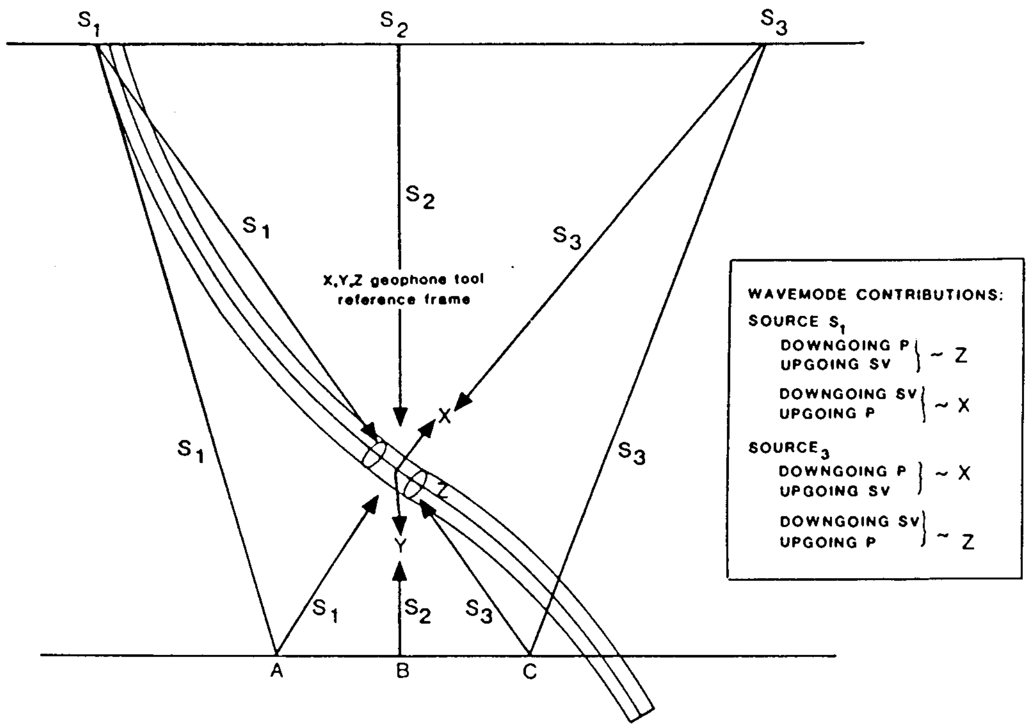

Figure 1.11 For the case of a deviated borehole, the triaxial geophone package receives contributions of P-, SV-, and SH- waves on all geophones. Even for the "near-offset" source location at S_2, the Z channel data will not contain P waves only. To separate the various wavefield contributions, the data on the three geophones are numerically rotated using hodogram polarization analysis. This is the "theoretical" geometry used in the analysis of the upgoing rays for the deviated borehole. Note that the upgoing rays travel very different directions when the subsurface layers are not horizontal as in Figure 1.1 (from Hinds et al. 1989a).

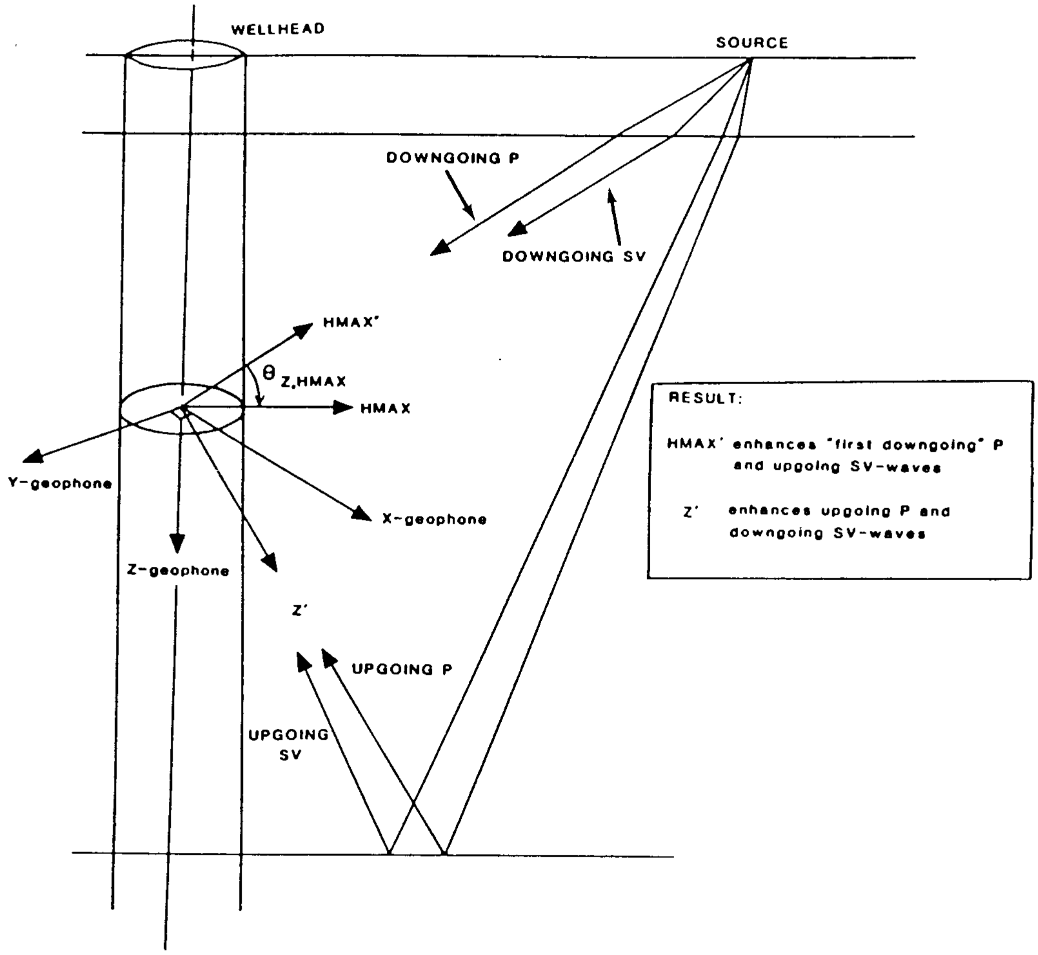

Figure 1.12 The geometry for time-variant rotations. To use the "classical" non-time variant rotations, it is assumed that the **HMAX'** data contain downgoing P- and upgoing SV-wave events only and that the **Z'** data contain upgoing P- and downgoing SV-wave events only. For the **Z'**, **HMAX'** rotation, the polarization analysis is performed on the downgoing primary wavelet (a single angle is chosen per VSP depth trace). The time-variant analysis consists of calculating the changing incidence angles of the upcoming P-wave (or SV) with increasing traveltimes at a single geophone location. The angle for a single layer is shown in the diagram whereas an entire model is input into the calculations which necessitates the time-variant calculation as the upgoing reflection angles change with each new layer used. For a single VSP trace, the angles are interpolated between the calculated model-based (time, angle) pairs to give a (time, angle) pair for each time sample following the first break for that trace (from Hinds et al., 1989a).

the application of normal move-out (NMO) corrections, VSP-CDP (Dillon and Thomson, 1984) mapping and migration techniques. However, as is shown in chapter 2, the **HMAX'** data contain residual upgoing P-wave energy. The angle of the upcoming P-wave recorded on a far offset VSP from the reflection off an interface just below the sonde will be different to the angle from an upgoing P-wave that resulted from a reflection from a much deeper interface. The angle of reflection from the deeper reflector (the angle between the vertical and the downgoing P-wave) will be smaller than the reflection from the shallower interface (both interfaces being below the sonde location).

A time-variant polarization of the upgoing events on given set of **Z** and **HMAX** traces can be performed by windowing the upgoing events and performing hodogram analysis of each event. However, due to the low amplitudes involved in the upgoing events, a model-based system is used to evaluate the time-variant polarization angles (time and angle pairs).

A model of the interfaces is constructed using the near offset first break times and ray-tracing is performed to given sonde model locations. The reflections from the various interfaces recorded at a given geophone location will result in (time, incidence angle) pairs from the modelled upgoing raypaths. These pairs are interpolated to provide a time-variant rotation angle for every time sample for the recorded trace at the same depth as the modelled geophone location. A time-variant polarization of the upgoing wave data from the **Z** and **HMAX** panels yields the **Z"** and **HMAX"** data panels as shown in chapter 2. The **Z"** data are then interpreted and correlated with the surface seismic.

The interpretive processing described in the next chapter drives the quality control decisions that will allow interpretation to evaluate every step of the processing.

For far offset data, the downgoing waves separated from the HMAX' panel are used to deconvolve the final **Z"** data. The constant time delay between the up- and downgoing multiples are assumed to exist; however, are these important time delay relationships valid for far offset data ? Figures 1.13 and 1.14 show the VSP modelled results (**Z** data) from a 980 m deep modelled borehole for the source offsets of 0, 200 400, 800, and 1000 m for surface-generated and interbed multiples, respectively. At far offsets, both the surface-generated and interbed multiple and primary up- and downgoing waves begin losing the simple time delay relationships found between the primaries and multiples found in the near offset VSP data. In chapter 2 and 6, a data example is given where a 524 m offset VSP was deconvolved with satisfactory results.

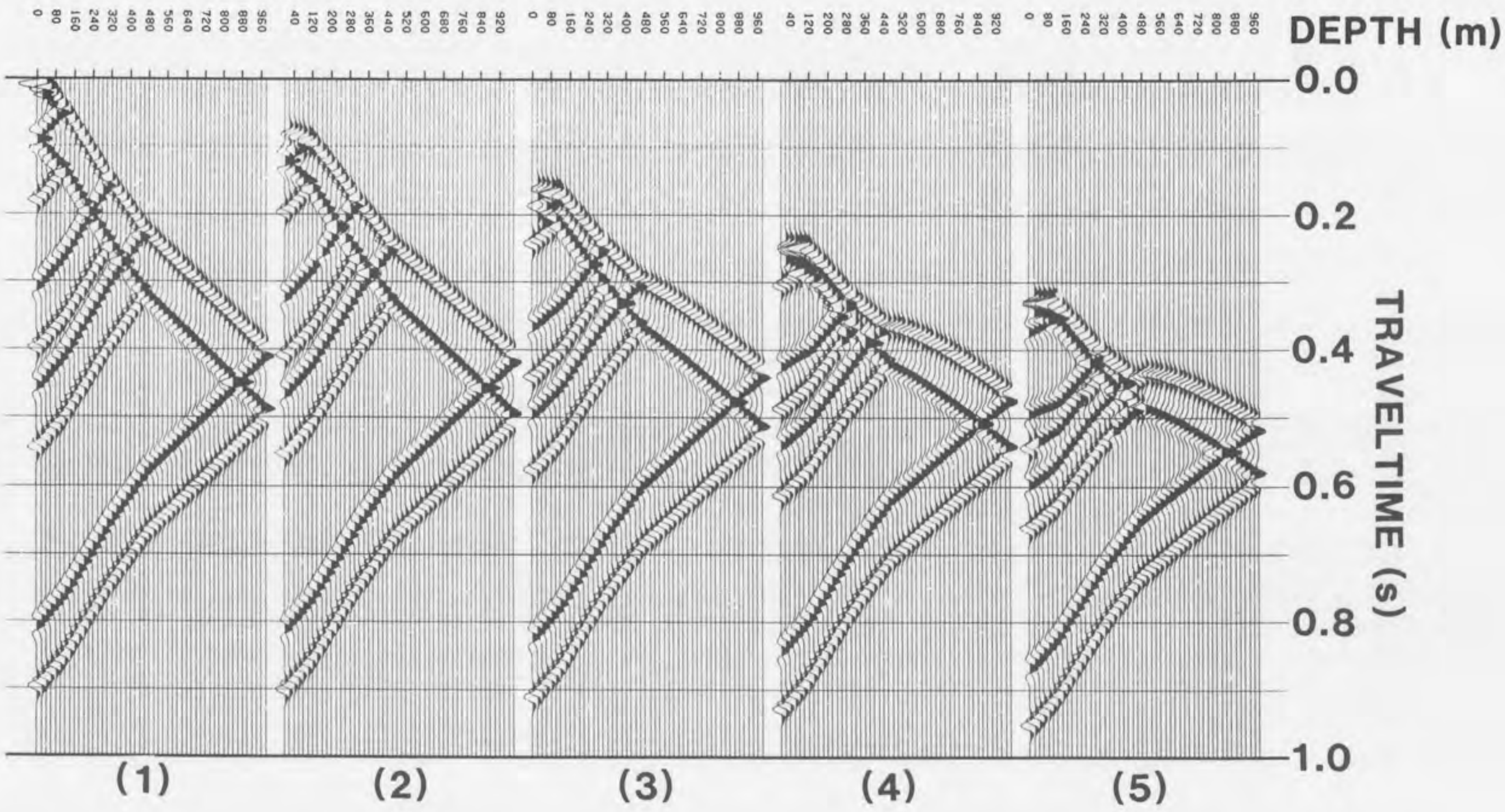

Figure 1.13 Synthetic VSP seismograms for the up- and downgoing primary and surface-generated multiple events for offsets of 0, 200, 400, 600 and 800 m (panel 1-5, respectively). The panels illustrate that the simplistic near offset primary-multiples time delays become complicated and invalid with increasing offset. The simple time delays between primary and multiple events (for near offset geometries) assume that the up- and downgoing wave propagation paths are vertically up and down, respectively. This relationship breaks down for far offset geometries.

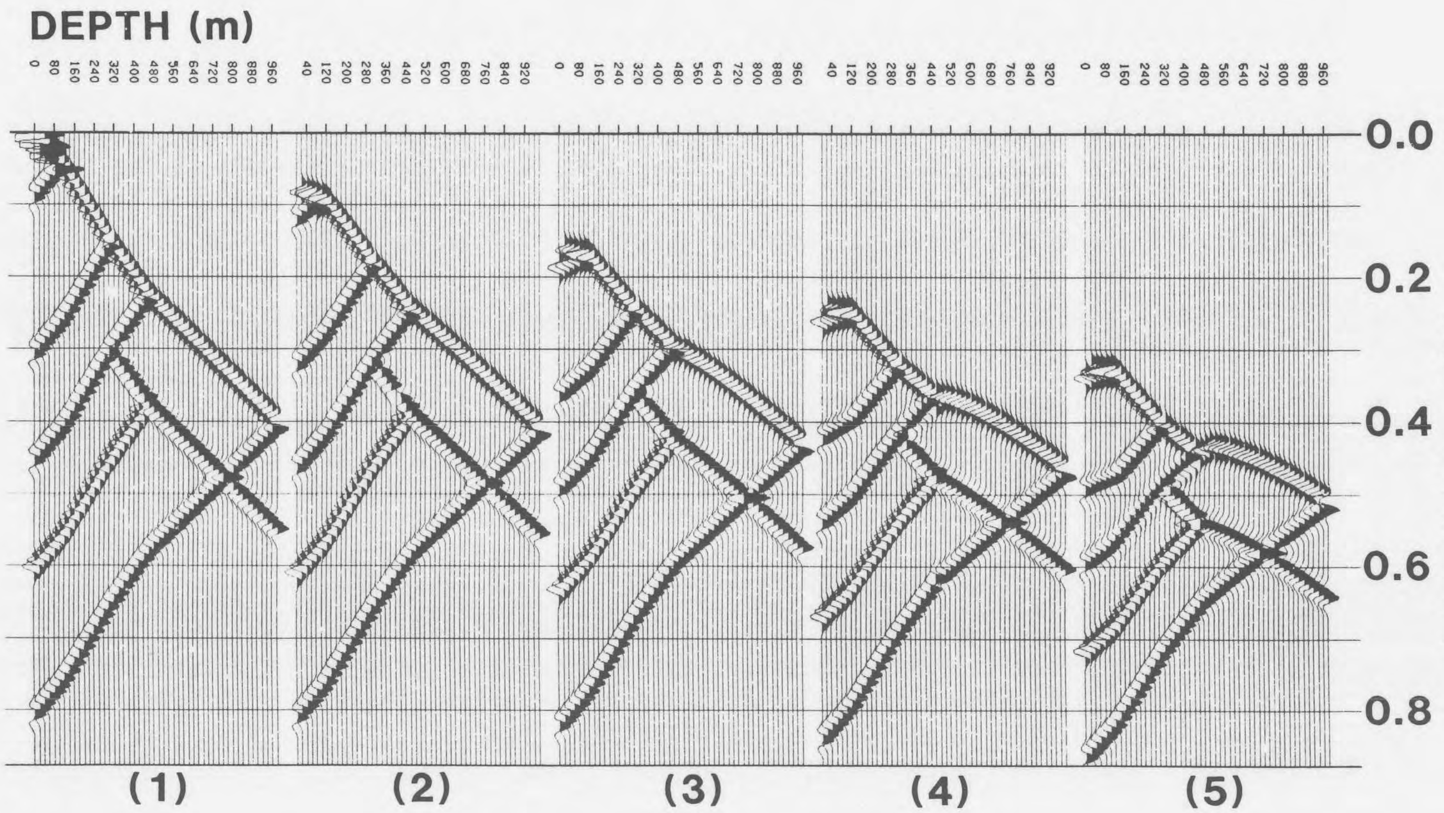

Figure 1.14 Synthetic VSP seismograms for the up- and downgoing primary and interbed generated multiple events for offsets of 0, 200, 400, 600 and 800 m (panel 1-5, respectively).